NON-SEISMIC GEOPHYSICAL MODELLING METHODS FOR REALISTIC CHARACTERISATION OF 3D GEOLOGY IN GREENFIELDS EXPLORATION: A CASE STUDY FROM THE SOUTHERN CARNARVON BASIN, AUSTRALIA

Helen Gibson*
Chloe Burney*
Desmond FitzGerald*
Matt Zengerer*

ABSTRACT

Innovative processing of high-resolution aerial geophysical survey data (gravity, magnetic and gravity gradiometry) combined with minimal geological data can constrain and validate realistic 3D geology models. In this way, exploration programmes in pre-3D seismic survey phases can access relatively low cost data acquisition and interpretation methods to facilitate detailed geological and structural interpretation, and thus elucidate spatial locations of source rocks, reservoirs, and potential sites for hydrocarbon traps.

Our case study focuses on the Merlinleigh Sub-basin, part of the southern Carnavon Basin in Western Australia (Figure 1). For this project we built an initial 3D geology model constrained by minimal geological mapping and just two interpreted regional seismic sections. (Alternatively, a couple of deep stratigraphic wells could have been used.) Next we refined and validated the model using enhanced processing workflows applied to potential field data, including multi-scale edge detection, and depth to basement determination. Finally, we applied a stochastic geophysical inversion to explore for all valid alternative models which can honour the independent datasets (geology, gravity and magnetics) and determined the most probable geological and rock-property models, via a Markov Chain Monte Carlo approach.

Model validation prompted the following key geological findings: (i) Multi-scale edge detection outcomes supported the geological modelling, and were particularly useful for mapping of the Wandagee and Kennedy Faults in 3D; (ii) Depth to basement processing concurred with the available seismic section data, and enabled extension of the top of basement mapping in 3D away from the limited seismic lines available. (iii) Property optimisation revealed a high density dyke-like formation aligned with the Wandagee Fault and within basement; and (iv) The most-probable geological model from the post-inversion outcomes indicated small refinements to the geology-geometry mainly to the top of basement horizon compared with the advanced starting model.

Our study demonstrates it is possible to accurately characterise 3D geology in greenfields exploration areas by acquiring relatively low cost potential field data, and applying innovative processing and 3D modelling techniques.

Keywords: 3D geology, airborne magnetics and gravity, multi-scale edge enhancement (worming), spectral depth determination, Murthy and Roa depth to basement, litho-constrained stochastic inversion.

INTRODUCTION

The Merlinleigh Sub-basin forms part of the onshore southern Carnavon Basin in Western Australia. This Phanerozoic basin is elongated approximately north-south, and staddles the Western Australia coast. In the region of the Merlinleigh Sub-basin (Fig. 1) Proterozoic basement is overlain by up to 7km of mainly Permo-Carboniferous sedimentary successions and a thin Mesozoic sequence (Iasky et al., 1998). These units thicken towards the north and west, and are also folded and dissected by faults which trend north-south and northwest-southeast. The Merlinleigh Sub-basin is flanked to the east by Archaen Pilbara Craton, and to the west by the Gascoyne Sub-basin.

The structural evolution of the southern Carnarvon Basin spans the Ordovician to Late Permian. Beginning as an epicratonic rift basin, shallow

---

*   **Intrepid Geophysics, Melbourne Australia**

marine conditions prevailed by the Late Silurian and ceased in the mid-Carboniferous due to significant compressional tectonics, accompanied by uplift and erosion of most of the sub-basin and the adjacent Pilbara Craton. Rifting recommenced in the Late Carboniferous to Early Permian initiating a second phase of deposition, and activating the main north-south trending faults of the Merlinleigh Sub-basin: the Wandagee and Kennedy Faults (Iasky et al., 1998).

Unlike the productive northern Carnavon Basin, the southern Carnavon Basin has to date only revealed minor gas shows, through the drilling of about 30 exploration wells. Source rock data is sparse, but characterised as excellent and gas-prone in the Lower Permian and oil-prone in the Lower Ordovician, Upper Devonian, Lower Carboniferous and Upper Permian. Reservoir targets exist throughout the Ordovician, Devonian and Permian sandstones. More detailed exploration is still required to confirm the hydrocarbon potential of the southern Carnavon Basin.

POTENTIAL FIELD DATA

In 1995, as part of a petroleum initiatives program, the Geological Survey of Western Australia acquired high-resolution aeromagnetic and semi-detailed helicopter-supported gravity surveys over the Merlinleigh Sub-basin to assist with interpretation and assessment of the hydrocarbon potential of this area. These geophysical datasets supplemented regionally spaced seismic sections (about 2000 line-km) acquired earlier by Esso in 1982–83.

Line data of the potential field surveys were gridded at a cell size equivalent to a quarter of the traverse line spacing (Figs. 2 and 3). The 1995 magnetic and gravity anomaly grids were used in the following workflows to achieve detailed geological interpretation and 3D mapping.

INTERPRETATION WORKFLOWS

Three processing and interpretation workflows were applied to the potential field data:

(1) Multi-scale edge enhancement (Worming)

Multi-scale edge enhancement ("Worming") is an automatic process of detecting linear contacts along maximum gradients in either gravity or magnetic data which can be applied at different upward continuation levels of the same data (Hornby et al.,

1999). On each level the isolated linears can be grouped to form 'worms'. When depth-corrected by Euler/Naudy Deconvolution methods to estimate their signal sources (FitzGerald et al, 2004), the location and shape of worms compiled in 3D is a function of the 3D subsurface geometry of rocks with contrasting properties (Holden et al., 2000). These methodologies can aid subsurface geological and structural interpretation directly from potential field data.

Worming of both the gravity and magnetic datasets from the Merlinleigh Sub-basin was carried out to discover the spatial extents of the edges of geophysical anomalies, and thus to aid structural interpretation (Figure 4).

(2) Spectral depth determination

Using the power spectrum of the gridded gravity data, residual anomalies (shallower depth sources) were filtered from the regional anomalies to isolate the signal from deeper sources (Spector and Grant, 1970). The two separate output grids (Fig. 5) were used to distinguish the signal from basement, from the signal from the sedimentary cover. The residual grids were also used later to test the geophysical inversion outcomes.

(3) Murthy and Roa depth to basement technique

This gravity inversion technique (Murthy & Rao, 1989) was used to determine a depth estimation to the top of basement in the Merlinleigh Sub-basin. The resulting depth contour grid was used to refine the 3D geological model.

3D Geological and Geophysical Modelling Workflows

An initial 3D geology model of the Merlinleigh sub-basin was rapidly built (Fig. 6.). It was constrained by surface geology mapping data, interpreted regional seismic sections, and the depth contour grid resulting from the Murthy and Rao technique. This model is geolocated and incorporates the SRTM 90m data (CGIAR-CSI) to constrain topography.

This initial 3D geology model was later refined and validated again using the gravity and magnetics datasets during a litho-constrained stochastic inversion. But in preparing for the inversion run, both rock property optimisation, and forward geophysical modelling formed part of the workflow.

(4) Rock property optimisation

Existing datasets for measured densities and magnetic susceptibilities for each geology formation in the Merlinleigh Sub-basin are sparse or non-existent, hence much uncertainty surrounded these values for modelling purposes. Therefore, our first step required running property optimisations referenced against the initial geology model, and the potential field data. Results of the magnetic property optimisation revealed a predominant magnetisation of the basement, as expected. Results of the density optimisation (Fig. 7) interestingly showed a high density body (around 2.8 gcm^{-3}) along the Wandagee fault, and located in basement which has a contrasting average density of 2.65 gcm^{-3}.

Based on this key result, the original geology model was modified and an intrusion of density 2.82 gcm^{-3} was introduced along the fault in the basement zone.

[Note that property optimisation, forward modelling and inversion are all performed on a discretised version of the smooth 3D geology model (Figure 7). This step creates a 3D grid or "voxel" model, necessary for computation purposes, and storing outcomes for later interrogation.]

(5) Forward geophysical modelling 2D and 3D

Before starting a full 3D inversion, the geological model was tested against the observed magnetic and gravity data in a series of 2D and 3D forward modelling runs. This enabled model refinement (either by modifying the rock properties or geology geometries), and then repeating of forward modelling in an iterative manner (Figure 8).

The aim is to achieve a fairly close starting model, prior to commencing inversion. This geology model and associated rock properties assignments will ideally reproduce the main features of the observed geophysical datasets.

(6) Litho-constrained stochastic geophysical inversion

There are always variations to a 3D geology model that still honour the observed data (geological contacts & structural data), and there are still more geological models that can reproduce the observed potential field data. This non-uniqueness encountered when modelling nature is important to keep in mind because if we were returned a single optimal model-solution to a inversion case study, this would neither be every useful or realistic. So rather than a deterministic geophysical inversion, we rather adopt a Bayesian approach (Markov Chain Monte Carlo), and thus access a statistical distillation of all plausible model-solutions which can honour the independent constraints from geology, rock property distribution laws, and observed potential field data (McInerney et., al., 2005).

At the commencement of inversion, each cell of the starting model is attributed with a lithology identity, a density value and a magnetic susceptibility value. (Properties are either sampled from user-set distribution laws, or prescribed in a customised property distribution.) During inversion, a modification is made to one cell at a time, either in terms of a geology-identity change, or a rock property change. The geophysical response of the perturbed model is computed, and then assessed against observed geophysics. If the misfit is better than for the last iteration, the model is kept. If the misfit is worse, the model is generally (but not always) rejected.

Rather than iterations ceasing when misfits reach a user-specified low limit (this would be a deterministic approach), the inversion continues to iterate, exploring millions of possible models which honour all independent data sets. Statistical distillation of all these possible models forms the basis of the inversion outcomes which are reported here in terms of probabilities.

Litho-constrained stochastic geophysical inversion as described here, was applied to the advanced 3D geological model built for the Merlinleigh Sub-basin.

Key Geological Findings:

a) Worming of both the gravity and magnetic datasets from the Merlinleigh Sub-basin was carried out to discover the spatial extents of the edges of geophysical anomalies, and thus to aid structural interpretation. Results supported the geological modelling, and were particularly useful for mapping of the Wandagee and Kennedy Faults in 3D.

b) The depth to basement contour grid estimated using the Murthy and Roa technique concurred with the available seismic section data, and enabled extension of the top of basement

mapping in 3D, away from the limited seismic lines available.

c) Property optimisation revealed a high density dyke-like formation aligned with the Wandagee Fault and within basement. This feature was added to the geological model during model-refinement.

d) Litho-constrained stochastic geophysical inversion delivered most probably models for related variables of geology-geometry and rock properties. Generally speaking, the inversion did not drive significant changes to the already well-refined starting model. However, minor changes were notable in the top of basement structure.

CONCLUSION

This case study of the Merlinleigh Sub-basin demonstrates that it is possible to accurately characterise 3D geology in greenfields exploration areas by acquiring relatively low cost potential field data, and applying innovative processing and 3D modelling techniques.

REFERENCES

Hornby, P., Boschetti F., and Horowitz F.G., 1999. Analysis of potential field data in the wavelet domain: Geophysical Journal International, **137**, 175-196.

FitzGerald, D., Reid, A., and McInerney, P., 2004, New discrimination techniques for Euler deconvolution: Computers & Geosciences, 30, 461–469.

Holden D., Archibald, N., Boschetti, F. and Jessell, M. 2000. Inferring geological structures using wavelet-based multiscale edge analysis and forward models. Exploration Geophysics (2000) 31, 617-621.

Spector, A., and Grant, F.S. (1970), Statistical methods for interpreting aeromagnetic data, Geophysics 35, pp 293–302

McInerney, P., Guillen, A., Courrioux, G., Calcagno, P. and Lees, T., 2005. Building 3D geological models directly from the data? A new approach applied to Broken Hill, Australia. Digital Mapping Techniques pp 119-130.

Murthy, I., V., R. and Rao, S., J., 1989, A Fortran-77 program for inverting gravity anomalies of two dimensional basement structures, Computers and Geosciences, 15 (7), 1149–1156.

Iasky, R. P., Mory, A. J., Ghori, K. A. R., and Shevchenko, S. I., 1998, Structure and petroleum potential of the southern Merlinleigh Sub-basin, Carnarvon Basin, Western Australia: Western Australia Geological Survey, Report 61, 63p.
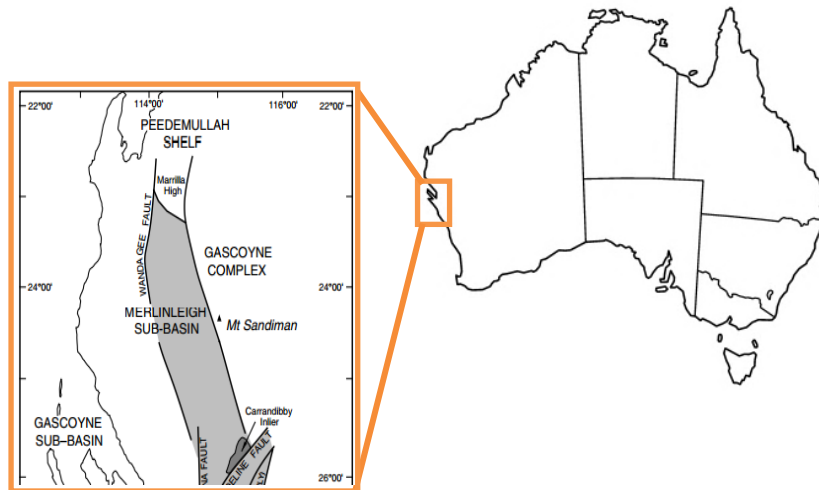
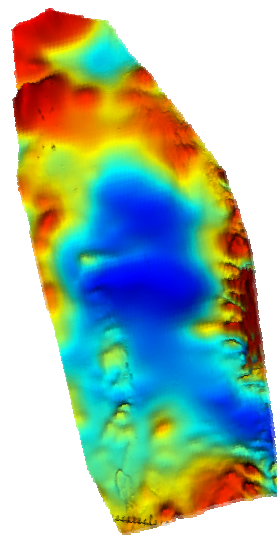**Figure 1** - Location of the Merlinleigh Sub-basin, Western Australia

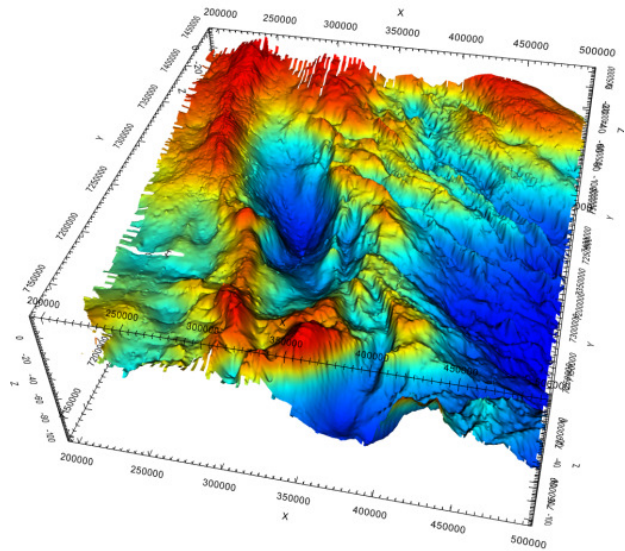**Figure 2** - Total Magnetic Intensity (TMI) grid for the Merlinleigh Sub-Basin (Cell size 106m)

Figure 3 - Terrain corrected scalar gravity anomaly grid for the Merlinleigh Sub-Basin (cell size 250m)
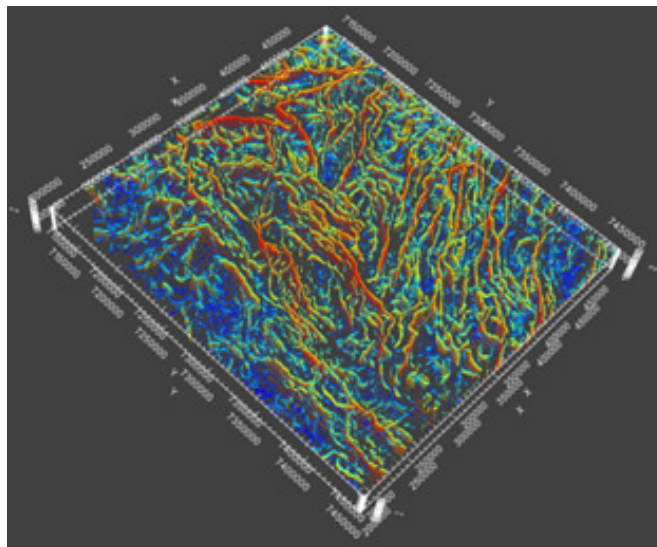

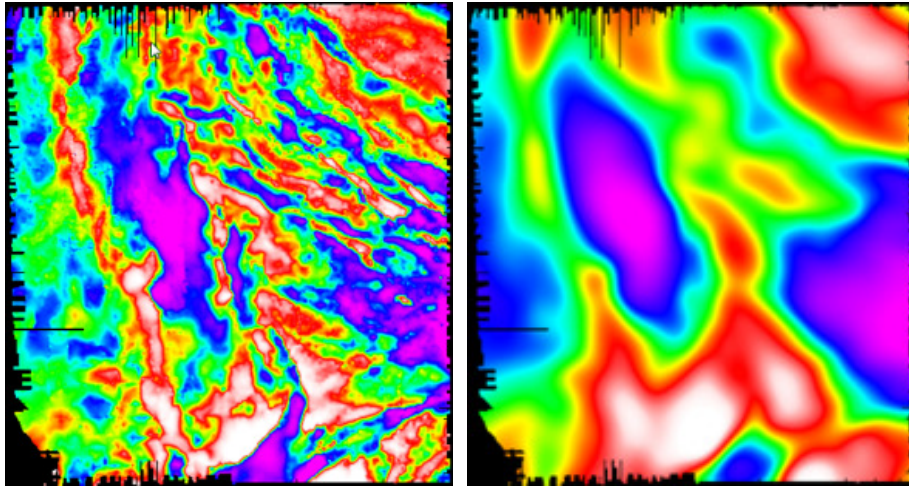**Figure 4** - 3D view of the gravity worms, Merlinleigh Sub-basin.

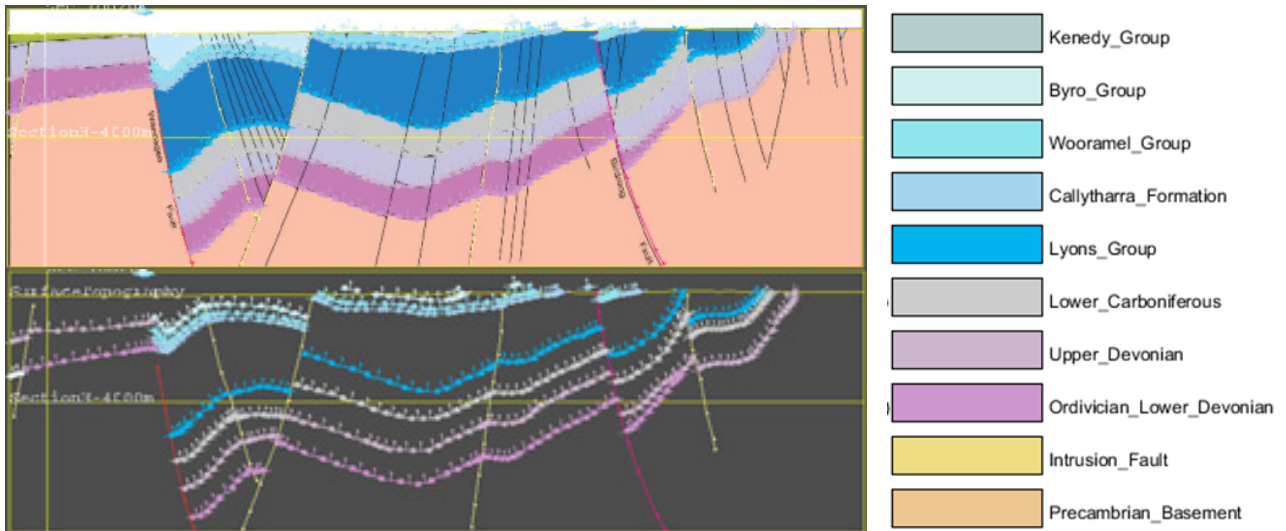**Figure 5** - Grids of the Merlinleigh Sub-basin gravity data. Left: residual signals, Right: regional signal.

Figure 6 - Upper: Interpreted seismic section (after Iasky et al., 1998) which was geolocated in GeoModeller, and used to digitize geological constraints (Lower) for the initial 3D geology model. Right: Stratigraphic pile for the Merlinleigh Sub-basin.
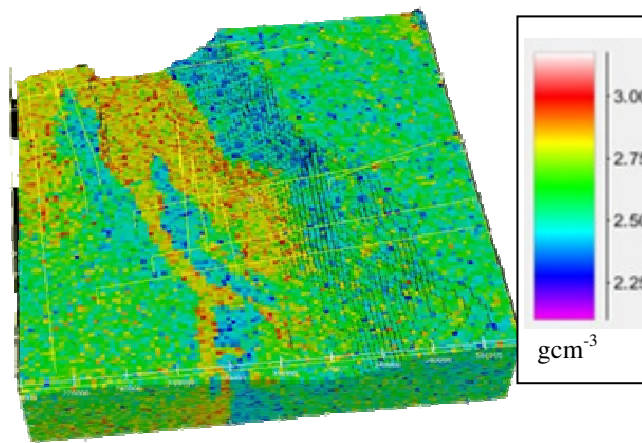
Figure 7 - Resulting block model of density for the Merlinleigh Sub-basin, after rock property optimisation. A key finding was the indication of a high density body (around 2.8 gcm^{-3}) along the Wandagee fault, located in the basement zone.
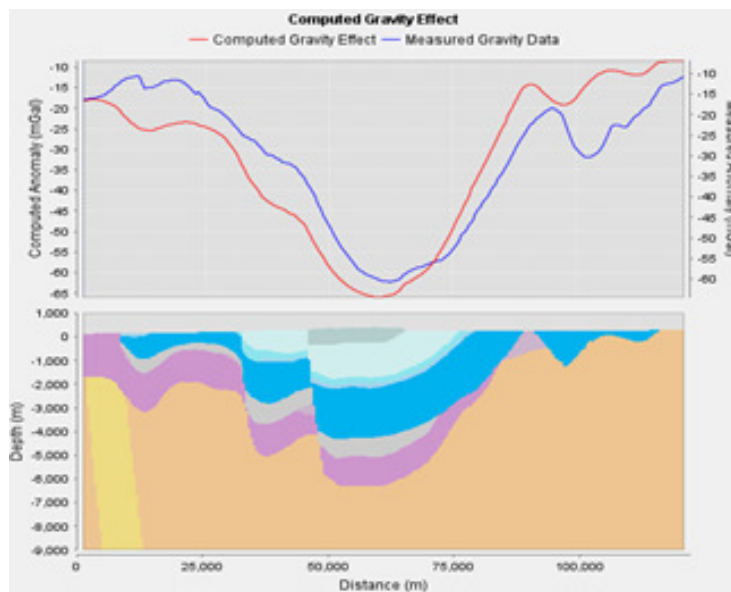

Figure 8 - Profile modelling (2D forward modelling) through the Merlinleigh Sub-basin 3D geology model, performed for the purpose of refining the model, prior to 3D forward modelling, and full geophysical inversion. (A close model fitting all independent data sets is the best starting point for inversion.)
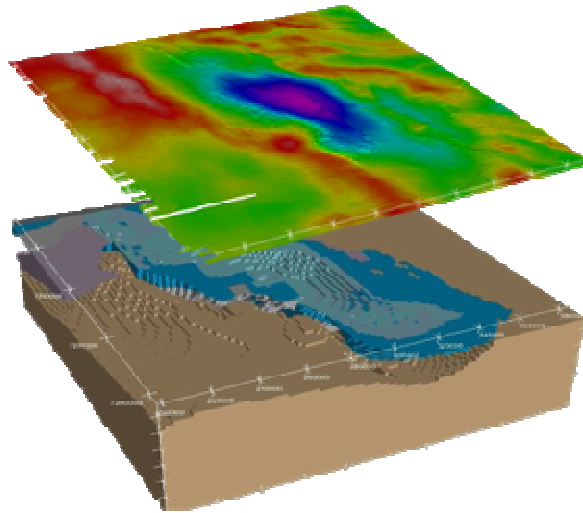
Figure 9 - Upper: Gravity anomaly grid. Lower: Discretised starting geology model (block model or "lithology voxet") of the Merlinleigh Sub-basin prior to inversion, with the basement visible.
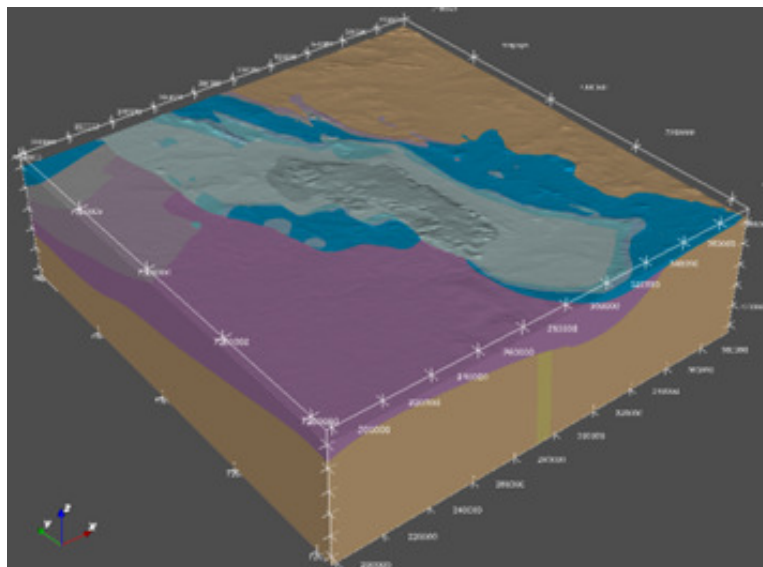

Figure 10 - The most-probable geological model of the Merlinleigh Sub-basin from the post-inversion statistical distillation of all possible models. A key outcome of the case study; this is the culmination of all applied processing and interpretation workflows.